

# Identification of Low Dimensional Chaos in Epileptogenic Seizure and Non-Seizure EEG using Solitary Wavelet Analysis

Sai Venkatesh Balasubramanian

*Sree Sai Vidhya Mandhir, Mallasandra, Bengaluru-560109, Karnataka, India.  
saivenkateshbalasubramanian@gmail.com*

---

## Abstract

The present work purports to the spectral and nonlinear analysis of intracranially recorded Electroencephalogram (EEG) time series data resulting in the identification and characterization of a low-dimensional chaos therein. Specifically, three categories of EEG time series data are considered: those recorded in non-epileptogenic regions during normal activity ('healthy' EEG), those recorded in epileptogenic regions during seizure activity ('Seizure' EEG), and those recorded in epileptogenic regions during normal non-seizure activity. In order to perform the spectral analysis efficiently, a new kind of wavelet, the solitary wavelet is proposed based on the hyperbolic secant function, where it is seen that this wavelet possesses vanishing higher moments with a negative logarithmic slope, thus translating to efficient detection of burst type signals without multiple levels of decomposition and reconstruction. The spectral analyses of the three categories of EEG data performed using Fourier and Wavelet analyses reveal that seizure EEG spectra, to a greater extent, and non-seizure epileptogenic EEG spectra, to a lesser extent, display prominent high frequency peaks, suggestive of resonant behavior. Nonlinear analysis using phase portraits too confirm the resonance oriented periodic orbits seen in Seizure EEG. Finally, quantitative analysis performed using Largest Lyapunov Exponents (LLE) and Fractal Dimension (D) reveal that both D and LLE values for seizure EEG are much lower than the healthy counterparts, with non-seizure epileptogenic EEG D and LLE values seen somewhere in between. The essence of these results is the observation of a distinct, uniquely identifiable low-dimensional chaotic behavior in EEG taken from epileptogenic region during non-seizure activities. This information can be used both as a preventive epilepsy diagnostic technique, as well as a post-surgical recovery assessment tool, and this forms the novelty of the present work.

*Keywords:* Electroencephalogram, Nonlinear Time Series Analysis, Epileptic Seizures, Solitary Wavelet, Lyapunov Exponents, Fractal Dimension

---

## 1. Introduction

The assertive signatures of Chaos Theory one of the defining highlights of twentieth century science are determinism and an extremely sensitive dependence on initial conditions. The observation of these signatures in recent times, arising out of nonlinearity and complexity have been possible, thanks to advancements in computer simulation and visualization technologies [1, 2]. Consequently, this has led to the application of chaos theory in diverse fields, including astrophysics, mechanics, engineering and secure communications [1]-[16]. However, the most significant application of chaos theory lies in enabling enhanced and thorough diagnosis of various pathologies in the human anatomy, owing to the identification of complexity and spatiotemporal patterns in biosignals such as the Electrocardiogram (ECG) and Electroencephalogram (EEG)[17, 18, 19].

In particular, Nonlinear Time Series Analysis (NTSA) techniques have been used in EEG based analysis, covering healthy recordings of sleep, rest, cognitive activity, influence of ethanol and other anaesthetics, as well as in pathological cases such as Alzheimer's, Parkinson's, depression and schizophrenia [20]-[32]. However, the NTSA application that has attracted the most attention is the analysis of EEG in epileptic pathologies [33]-[40]. Epileptic seizures are often a result of abnormally excessive synchronous neuronal activity in the brain, and are broadly classified as convulsive seizures, such as focal and generalized seizures, accounting for nearly 60 percent of seizures, and non-convulsive seizures, such as absence seizures (petit mal) accounting for the remaining 40 percent of seizures [41, 42, 43, 44].

It is a well-established fact that significant nonlinear behavior exists during seizures (ictal activity). Studies have been performed in literature comparing dynamical properties of brain electrical activity from different extracranial and intracranial recording regions, in different physiological and pathological brain states, with the general conclusion being that the agents producing epileptic seizure tend to drive brain activity toward stable periodic behavior, thus reducing the dimensionality of chaos. This physiologically translates to difficulty in information processing capabilities, though the

the low dimensionality of chaos is still sufficient to process reflex activities. However, most of the results thus concluded are centred on the pathological seizure EEG signal, compared with healthy EEG recordings during various stages of wakefulness and sleep [45, 46].

With the presence of chaos in EEG thus observed, the next step would be to perform more detailed characterization of the chaotic behavior, leading towards proper diagnosis and medication of various brain pathologies, and this forms the key motivation for this paper. Specifically, various EEG samples are taken from the Universitat Bonn - Klinik fur Epileptologie database, corresponding to three cases - healthy intracranial EEG taken from non-epileptogenic area, healthy intracranial EEG taken from epileptogenic area, and seizure affected EEG, and nonlinear analyses are performed for 100 samples from each category [45]. The analyses consist of qualitative and quantitative analyses. In qualitative analysis, the Fourier Analysis is performed, indicating spectral features of seizure activity and healthy activity EEG signals, following which multispectral resolution analysis is performed using wavelets. For this purpose, a new wavelet, termed the Solitary Wavelet is formulated based on the hyperbolic secant function, and it is seen that this wavelet has vanishing higher order moments with negative logarithmic slope, which results in efficient detection of burst-type signals, without introducing additional oscillations, and thus, without the need for multiple stages of decomposition and reconstruction. Following this, the phase portrait of the the categories are plotted. The quantitative analyses consist of two key tools to characterize chaos - the Fractal Dimension, a measure of the dimensionality of chaos, and the largest Lyapunov Exponent, a quantitative measure of the sensitive dependence on initial conditions. From all the analyses, it is clearly seen that healthy EEG signals are more complex and more chaotic than the seizure affected signals, agreeing with established results in literature.

However, the key highlight of the results reported in the present work is that the nonlinear analyses of the intracranial EEG taken from the epileptogenic hippocampal area, during healthy (non-seizure) activity show a decrease in chaotic behavior compared to intracranial EEG taken from the non-epileptogenic hippocampal area during healthy activity. This trend can be used effectively either as a predictive or post-surgical sign of epileptic seizures even when recording EEG signals during non-seizure activity, enabling one to resort to timely medication, such as anticonvulsants, and this forms the novelty of the present work.

## 2. Methodology

### 2.1. Electroencephalogram Data

The EEG time series data used in the present work are obtained from the Bonn University Klinik fur Epileptologie website [45],

([http://epileptologie-bonn.de/cms/front\\_content.php](http://epileptologie-bonn.de/cms/front_content.php))

. The EEG recordings obtained in this database are grouped into five categories as follows:

1. Dataset Z - Surface EEG of healthy volunteers, relaxed in an awake state, with eyes open.
2. Dataset O - Surface EEG of healthy volunteers, relaxed in an awake state, with eyes closed.
3. Dataset N - Intracranial EEG of patients, who had achieved complete seizure control, recorded in the non-epileptogenic hippocampal formation.
4. Dataset F - Intracranial EEG of patients, who had achieved complete seizure control, recorded in the epileptogenic hippocampal formation.
5. Dataset S - Intracranial EEG of patients during seizure activity, recorded in the epileptogenic region.

All EEG signals are recorded with 128-channel amplifier system, and after 12-bit analog to digital conversion, the data was acquired at a sampling rate of 173.61Hz, with a 12dB/octave band-pass filter at 0.53-40Hz [45]. All the analyses in the present work are performed using MATLAB.

### 2.2. Formulation of the Solitary Wavelet

A key part of the nonlinear analyses reported in this paper is the multispectral resolution analysis, carried out using wavelets. In the present work, the solitary wavelet, based on the hyperbolic secant function is used, and the formulation is as detailed below.

The first step is to define the Scaling Function, also called the ‘Father Wavelet’  $\phi$  in continuous time.  $\phi$  is defined as the hyperbolic secant  $sech(t)$  ( $\phi(t) = sech(t)$ ) [47, 48, 49]. The choice of hyperbolic secant is dictated by the fact that hyperbolic secant solitons are known to be very smooth, compact functions, making them ideal choices for a wavelet [50].

The Solitary Father Wavelet  $\phi$  thus defined is used as the basis to form the Solitary ‘Mother Wavelet’  $\psi$ , such that the following criteria are satisfied [47, 48, 49]:

1.  $\psi(t)$  belongs to a subspace of the space  $L^1(\mathbb{R}) \cap L^2(\mathbb{R})$ , the space of absolutely and square integrable measurable functions.
2.  $\phi(t)$  and  $\psi(t)$  are orthogonal to each other.
3.  $\psi(t)$  has zero mean, i.e. the following holds:

$$\int_{-\infty}^{\infty} \psi(t) dt = 0 \quad (1)$$

4.  $\psi(t)$  has unity square norm, as per the following equation:

$$\int_{-\infty}^{\infty} |\psi(t)|^2 dt = 1 \quad (2)$$

5. It is preferable, but not a mandatory criterion to ensure that  $\psi(t)$  possesses a higher number  $M$  vanishing moments. In other words, for all  $m < M$ ,

$$\int_{-\infty}^{\infty} t^m \psi(t) dt = 0 \quad (3)$$

The Solitary Mother Wavelet  $\psi$  is used to define the solitary daughter wavelets  $\psi_{a,b}(t)$  in the following fashion with  $a > 0$  denoting the ‘scale’ and  $b \in \mathbb{R}$  denoting the shift [47, 48, 49]:

$$\psi_{a,b}(t) = \frac{1}{\sqrt{a}} \psi \left( \frac{t-b}{a} \right) \quad (4)$$

The Father, Mother and Daughter Solitary Wavelets are then expressed as discrete signals  $\phi(n)$ ,  $\psi(n)$  and  $\psi_{a,b}(n)$  centered around zero.

Based on the above procedure, the solitary father and mother wavelets have been formed using the MATLAB Wavelet Toolbox. The Father and Mother Wavelet Signals are plotted in Fig. (1).

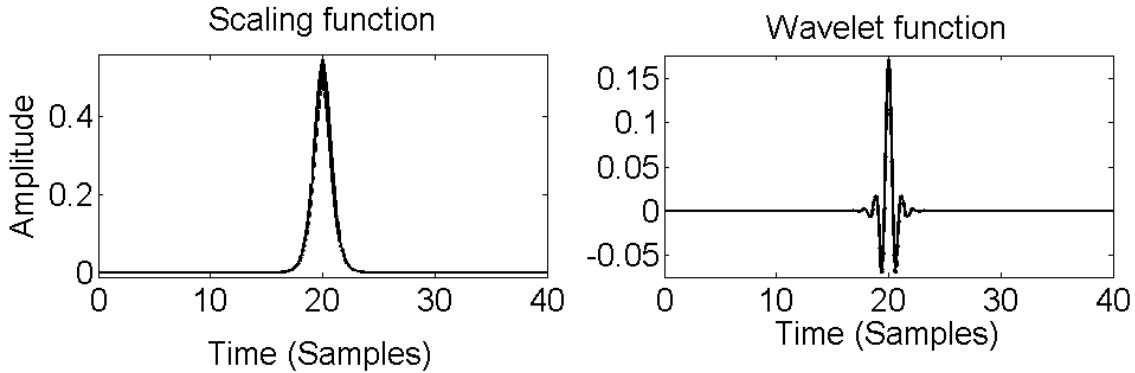


Figure 1: Father and Mother Signals of the Solitary Wavelet

Physically, the existence of vanishing higher moments signifies that the wavelet has a compact, continuous, smooth structure, and that the analysis of bursts in signals with such wavelets can be carried out with minimal filtering. In order to investigate and characterize the performance of the chaotic solitary wavelet, the moments upto the tenth order of the solitary mother wavelet (SOL) are computed and compared with the corresponding moments of six established wavelets, namely Daubechies 4 (DB4), Biorthogonal 4.4 (BIOR4.4), Reverse Biorthogonal 4.4 (RBIO4.4), Symlet 4 (SYM4), Coiflet 4 (COIF4) and the Discrete Meyer Wavelet (DMEY) [47, 48, 49]. The moments are tabulated in Table 1.

From Table 1, it is seen that the higher moments of the solitary wavelet tend toward zero. It is seen that even in the Meyer wavelet, known to exhibit vanishing moments up to very large orders, moments increase after a certain order (sixth). In order to better capture the trends of the higher moments, the moments of the various wavelets from the third order onwards are plotted on a logarithmic scale in Fig. (2). It is clearly seen that while all the other wavelet moments including those of the Daubechies and Meyer show an increasing trend, the solitary wavelet moments show a decreasing trend with a negative logarithmic slope. This indicates that the moments of the solitary wavelet rapidly decay and vanish toward zero. This gives the solitary wavelet the exclusive advantages of smoothness, compactness and thus inherent capability to detect burst type signals efficiently without the need for multiple levels of filtering and decomposition.

Table 1: Moments of Various Wavelets upto the Tenth Order

Moments	DB4	BIOR4.4	RBIO4.4	SYM4	COIF4	DMEY	SOL
First	0.00E+00						
Second	1.33E-01	1.09E-01	1.16E-01	1.33E-01	4.26E-02	9.90E-03	1.00E-02
Third	2.05E-02	5.41E-02	8.01E-02	6.96E-02	1.96E-02	3.30E-03	1.50E-03
Fourth	1.13E-01	9.95E-02	1.27E-01	1.30E-01	3.74E-02	7.60E-03	2.80E-03
Fifth	3.25E-02	8.78E-02	1.37E-01	1.14E-01	3.19E-02	5.40E-03	9.00E-04
Sixth	1.05E-01	1.12E-01	1.73E-01	1.52E-01	4.10E-02	7.30E-03	9.38E-04
Seventh	4.19E-02	1.16E-01	2.05E-01	1.58E-01	4.19E-02	6.60E-03	4.67E-04
Eighth	9.95E-02	3.45E-01	2.49E-01	1.90E-01	4.85E-02	7.60E-03	3.50E-04
Ninth	4.96E-02	1.47E-01	2.99E-01	2.08E-01	5.24E-02	7.60E-03	2.00E-04
Tenth	9.56E-02	1.66E-01	3.62E-01	2.42E-01	5.87E-02	8.30E-03	1.36E-04

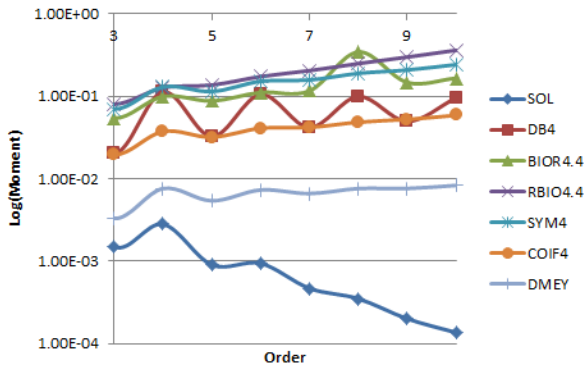


Figure 2: The Moments (upto Tenth Order) of Solitary Wavelets compared with contemporary wavelets on a logarithmic scale

### 3. Results and Discussion

#### 3.1. Spectral Analysis

The first stage of seizure and non-seizure analysis is the spectral analysis, performed by taking the FFT (Fast Fourier Transform) of the time series data, and this is plotted for 24 sample recordings in Fig. (3) for the non-seizure non-epileptogenic data (Dataset N), in Fig. (4) for the seizure data (Dataset S), and in (5) for the non-seizure epileptogenic data (Dataset F).

From the plots, one can observe the following inferences:

1. In most of the spectra of Dataset S corresponding to seizures, clear, well-defined, well-separated spectral peaks are seen, usually at x-axis values corresponding to 350 and 650, with such peaks rising to a significant extent above the central frequency component at 500. This trend suggests that, as mentioned before, epilepsy producing agents tend to drive brain activity towards periodic, often high-frequency resonance.
2. In the spectra of Dataset N, corresponding to healthy, non-epileptogenic EEG, the central frequency is clearly the highest peak, several orders of magnitude stronger than other frequency components, and in most cases, there is a clear absence of a second dominant peak. This means that the non-seizure healthy brain activity is almost evenly spread across a wide range of frequencies, thus contributing to a high degree of complexity and chaos.
3. The most interesting observation is in the case of spectra of Dataset F corresponding to non-seizure, epileptogenic region EEG, where it is seen that while there is a dominant central frequency as seen in the N spectra, but in addition to that, there are clear well-defined peaks, typically closer to the central frequencies (450 and 550), than is seen in the S spectra. Thus, the spectra of epileptogenic region EEG differ markedly from non-epileptogenic region EEG spectra, even during non-seizure activity.

In order to obtain a more enhanced spectral analysis, the multispectral resolution analysis is performed, using the Solitary Wavelet, as defined earlier. The shift-scale contour plot displaying solitary wavelet analyses results for 24 samples each of Datasets N, S and F are plotted in Fig. (6), Fig. (7) and Fig. (8) respectively.

From the FFT analysis presented earlier, it is but logical to infer that seizure EEG, to a greater extent and epileptogenic, non-seizure EEG to a lesser extent consists of high frequency components, with more localization of frequency

than in healthy EEG. In accordance to this observation are the wavelet analyses results. As seen from the plots, wavelet analyses of Dataset S are highly localized, with regions of dominance hardly exceeding scale levels of 8. This suggests that seizure EEG time series consist of pulses and peaks of very short widths. However wavelet analysis for Dataset N shows dominance that is not restricted to scales less than 8, but rather spread out over all scales. This is in direct accordance with the well-spread spectra seen earlier. However, wavelet analysis of Dataset F, indicates in some samples, localizations of dominant regions between scale values of 8 and 20, suggesting that epileptogenic non-seizure EEG comprises of pulses and peaks albeit with a larger widths than seizure EEG. The localized trends observed for the Datasets S and F are a testimony to the efficient burst-detection capabilities of Solitary Wavelet as described earlier, and this results in a more enhanced understanding of spectral behavior of all three EEG cases in multiple resolutions.

### 3.2. Nonlinear Analysis and Chaotic Characterization

The most important tool in nonlinear analysis of time series data is the Phase Portrait, which is a plot of a signal's time derivative in terms of the signal, illustrating the phase space dynamics and qualitatively serving as a tool to assess various chaotic parameters such as sensitivity and ergodicity [51]-[56]. Chaotic phase portraits are often characterized by well defined boundaries encompassing rich and ornamental patterns within them. The phase portrait analysis for 24 samples each of Datasets N, S and F are plotted in Fig. (9), Fig. (10) and Fig. (11) respectively.

From the plots, it is seen that phase portraits of seizure EEG follow almost regular, periodic orbits, which suggests a reduction in bandwidth and ergodicity, and this observation is in accordance with inferences obtained from Fourier and Wavelet analyses. The phase portraits of healthy EEGs are much more ergodic and rich, with the phase portraits of epileptogenic non-seizure EEG largely resembling those of healthy EEG. Thus, in the phase space dynamics, it is not in general possible to identify the seizure EEG-like localizations, unlike those seen in the Fourier and Wavelet Analyses.

Finally, quantitative nonlinear analysis of the EEG time series data can be achieved using two techniques:

1. The chaotic/fractal nature of the signal, termed its dimensionality is ascertained by computing the fractal dimension, using the Minkowski Bouligand Box Counting Method [57]. In this method, various square 'boxes' of different sizes  $e$  are formed and for each size  $e$ , the number of boxes  $N(e)$  required to cover the entire set is computed. The fractal dimension  $D$  is then given by

$$D = \lim_{e \rightarrow 0} \frac{\log(N(e))}{\log(e)} \quad (5)$$

2. The chaotic nature of the EEG signal is assertively established by calculating the largest Lyapunov Exponent (LLE), a measure of a system's sensitive dependence on initial conditions [58]. Rosenstein's algorithm is used to compute the Lyapunov Exponents  $\lambda_i$  from the time series, where the sensitive dependence is characterized by the divergence samples  $d_j(i)$  between nearest trajectories represented by  $j$  given as follows,  $C_j$  being a normalization constant [59]:

$$d_j(i) = C_j e^{\lambda_i(i\delta t)} \quad (6)$$

In each of the three datasets, N, S and F, the D and LLE values of 100 samples are computed and are averaged to give the averaged Fractal Dimension and Lyapunov Exponents of Healthy, Seizure and Non-Seizure Epileptogenic EEG as detailed below:

1. For Non-Seizure Non-Epileptogenic EEG (Dataset N), the D value is obtained as 5.02 with LLE value obtained as 4.34. This value of D is consistent with the one reported in literature [46].
2. For Seizure EEG (Dataset S), the D and LLE values obtained are 2.13 and 0.34, with negative LLE values observed for 27 of 100 samples. This is a clear assertion that seizure EEG's exhibit a far lesser degree of chaoticity than healthy EEGs with much lower dimensionality.
3. For Non-Seizure Epileptogenic EEG (Dataset F). the D value is obtained as 3.32, whereas average LLE value is 1.74. This implies that the sensitive dependence behavior of Non-Seizure Epileptogenic EEG is much more subdued than in case of Non-Seizure Non-Epileptogenic EEG, though with slightly higher chaoticity and dimensionality than Seizure EEG.

Thus, in summary, it can be concluded from both Spectral and Nonlinear Analyses results that seizure producing agents tend to drive brain activity towards a more resonant, high frequency, periodic/quasiperiodic behavior with much lower chaoticity and dimensionality than that of a healthy EEG, whereas in the case of Non-Seizure Epileptogenic EEG, one does observe these properties (resonance-oriented, high frequency, periodicity, lower dimensionality, lower LLE), albeit to a lesser extent than in seizure EEG data.

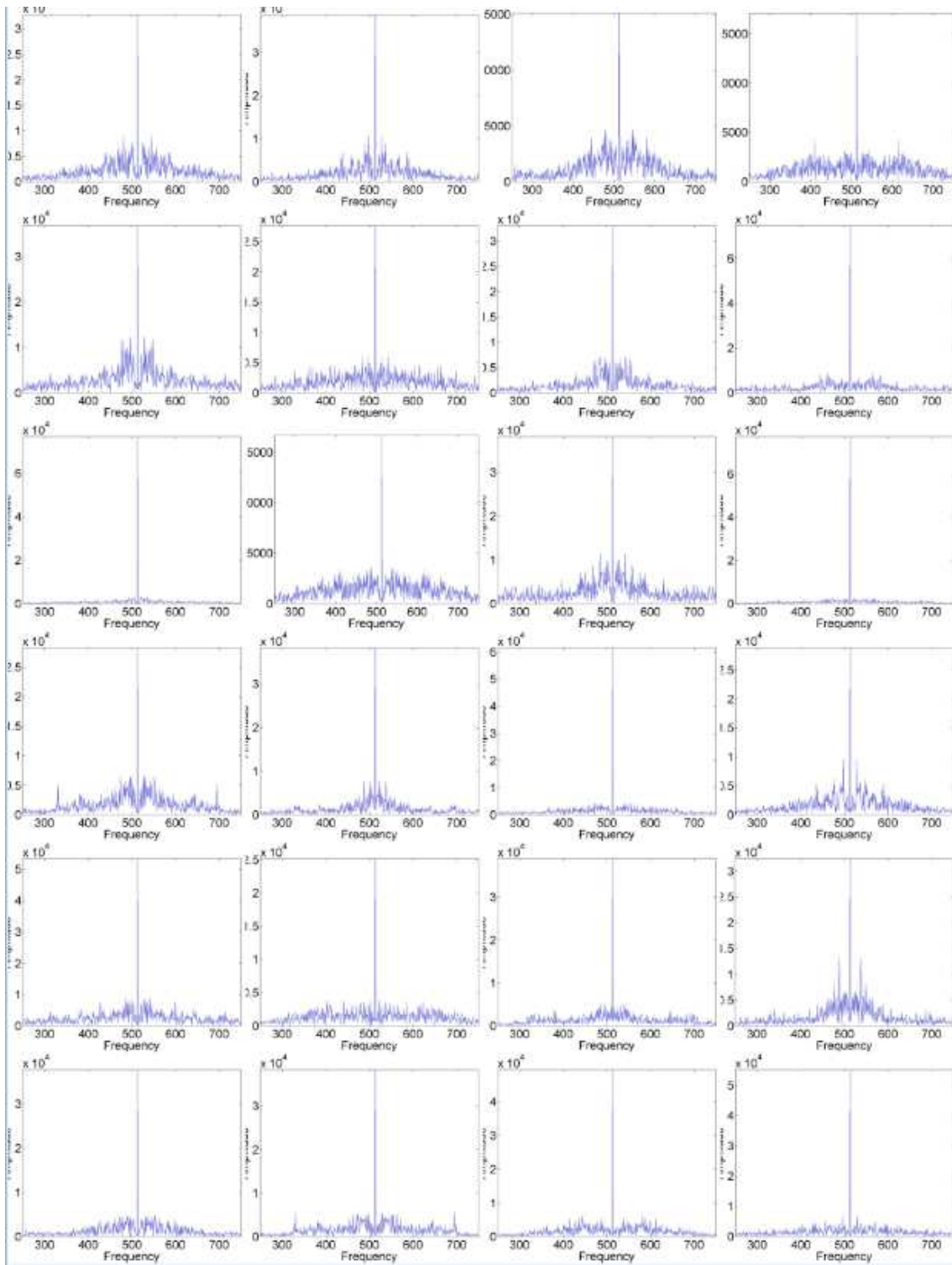


Figure 3: Spectral Analysis for 24 samples of EEG recorded during normal activity from non-epileptogenic region

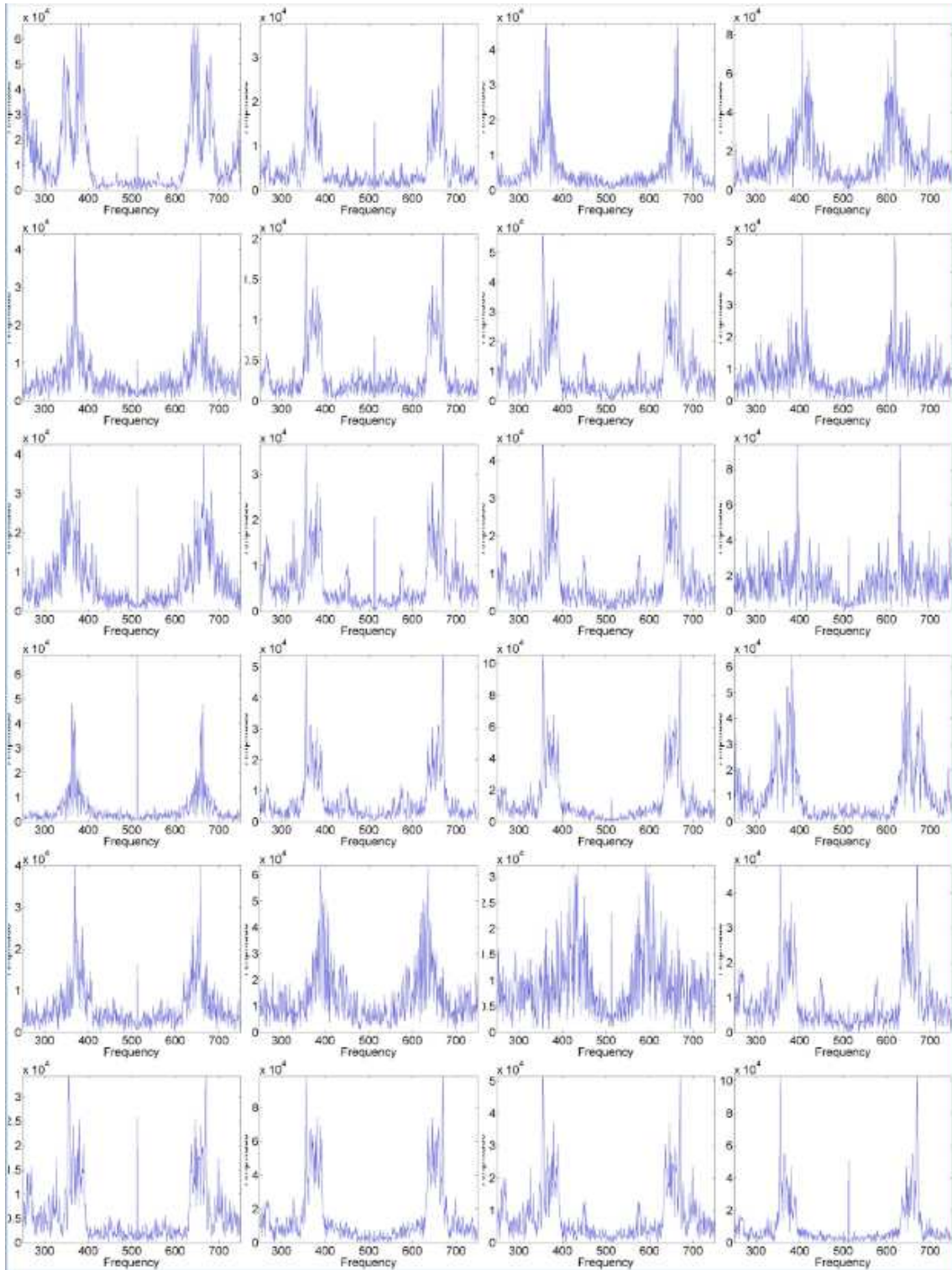


Figure 4: Spectral Analysis for 24 samples of EEG recorded during seizure activity from epileptogenic region

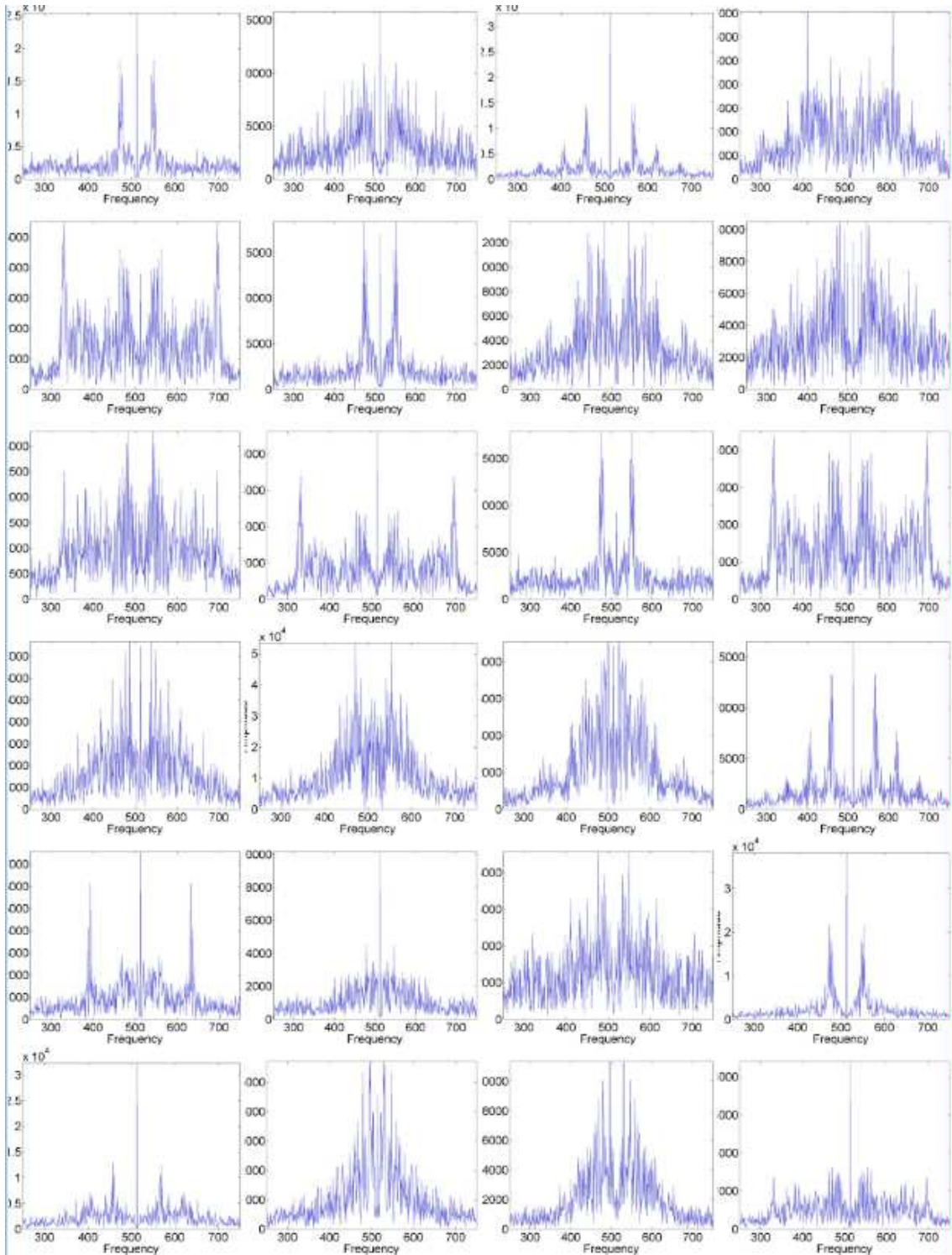


Figure 5: Spectral Analysis for 24 samples of EEG recorded during normal activity from epileptogenic region

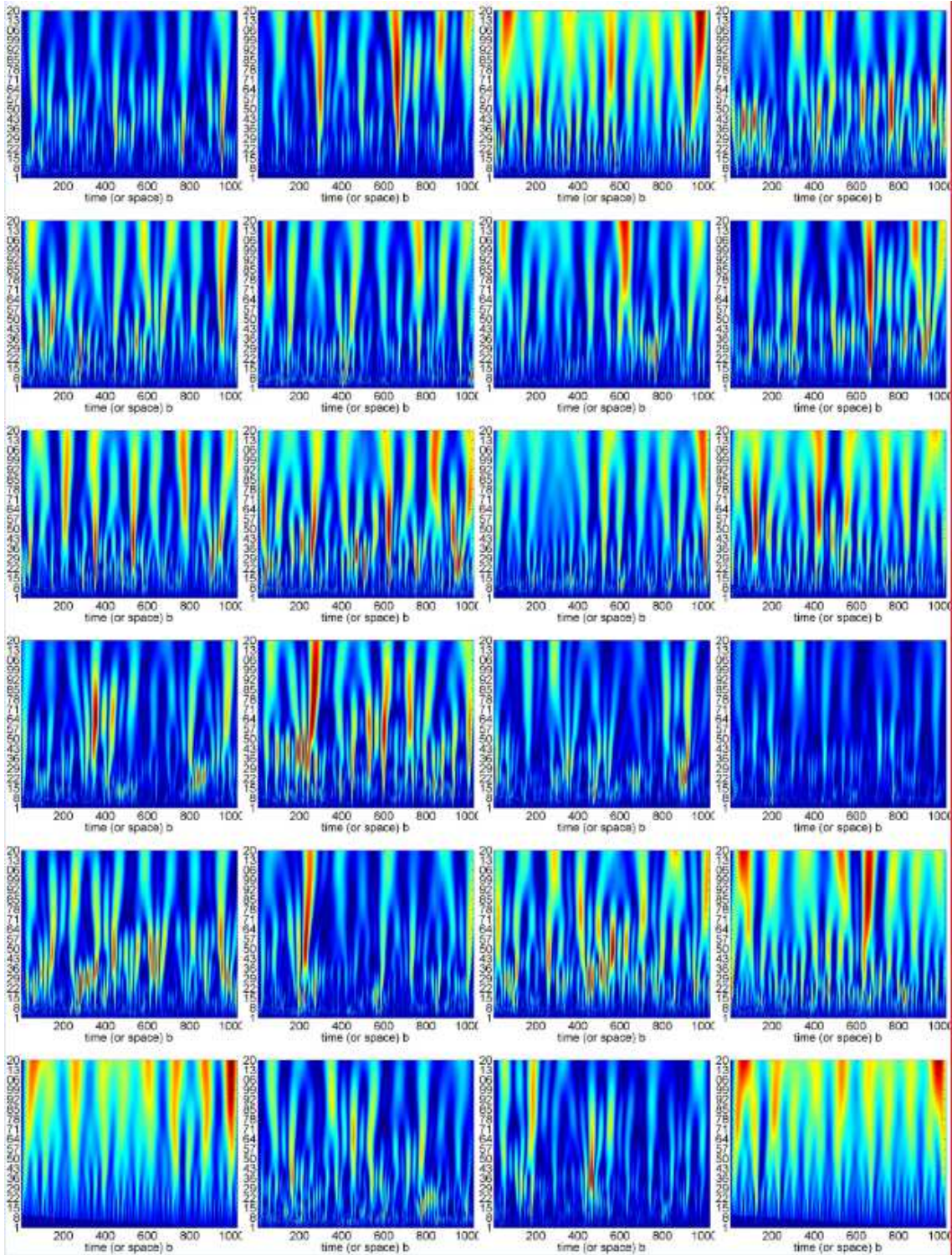


Figure 6: Solitary Wavelet Analysis for 24 samples of EEG recorded during normal activity from non-epileptogenic region

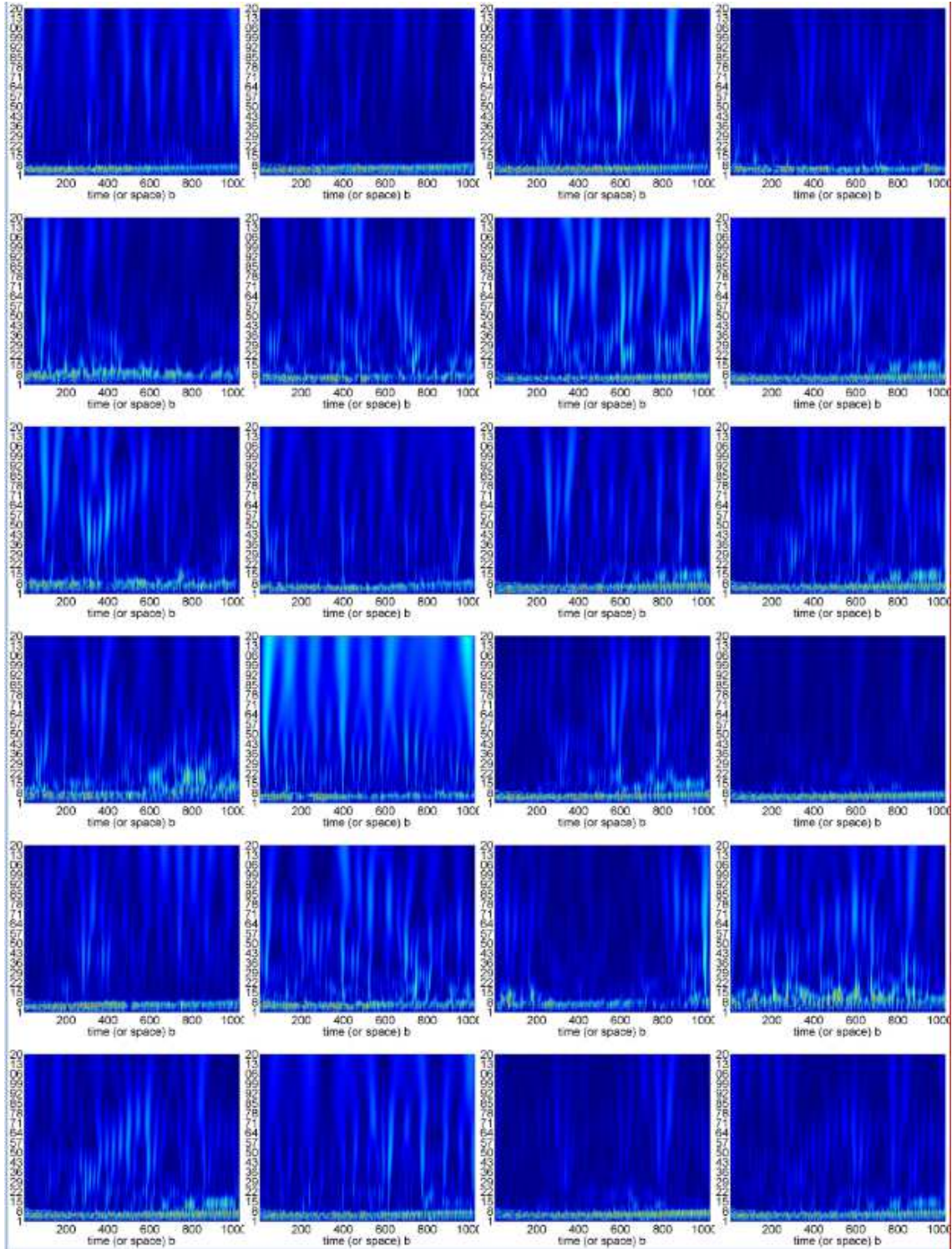


Figure 7: Solitary Wavelet Analysis for 24 samples of EEG recorded during seizure activity from epileptogenic region

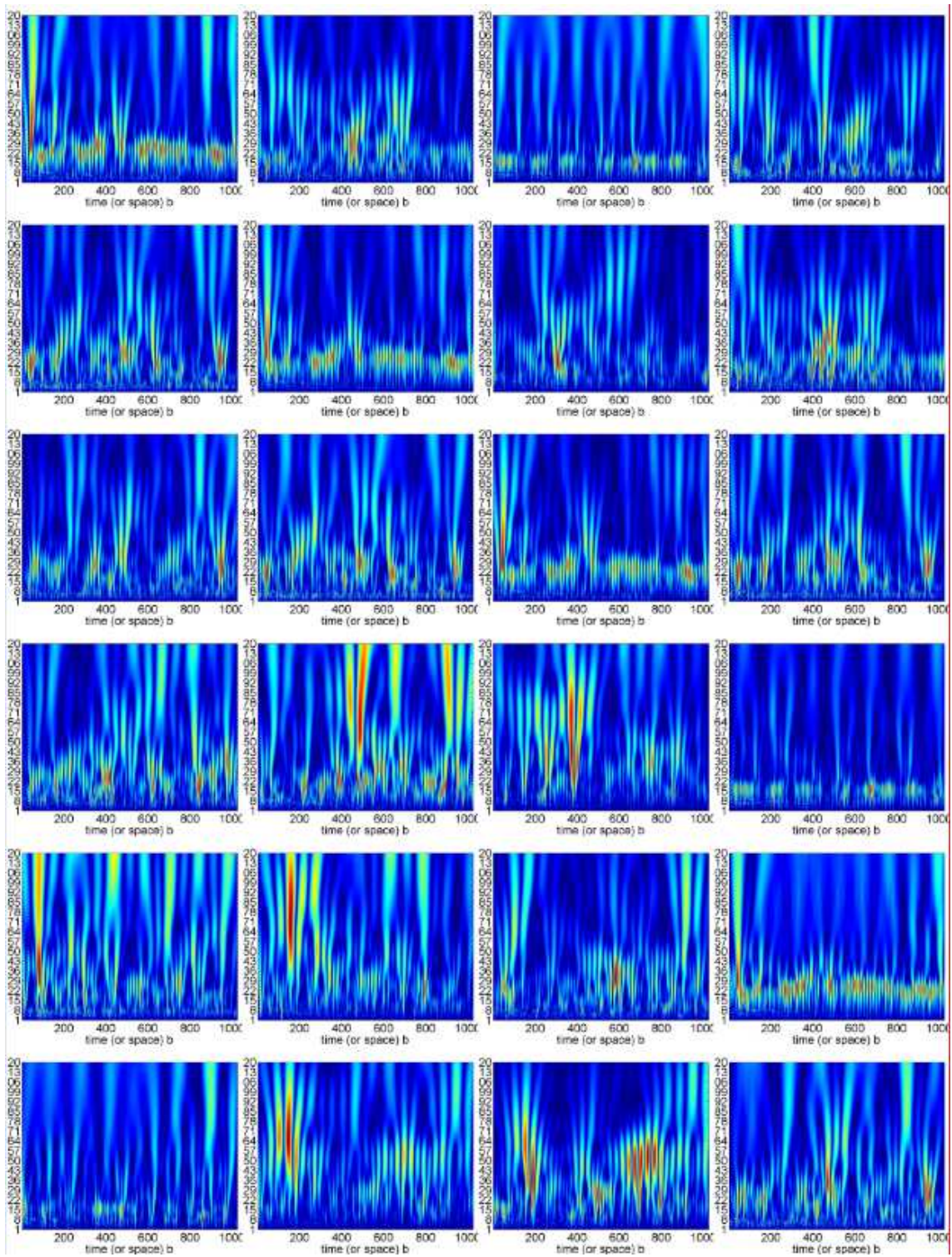


Figure 8: Solitary Wavelet Analysis for 24 samples of EEG recorded during normal activity from epileptogenic region

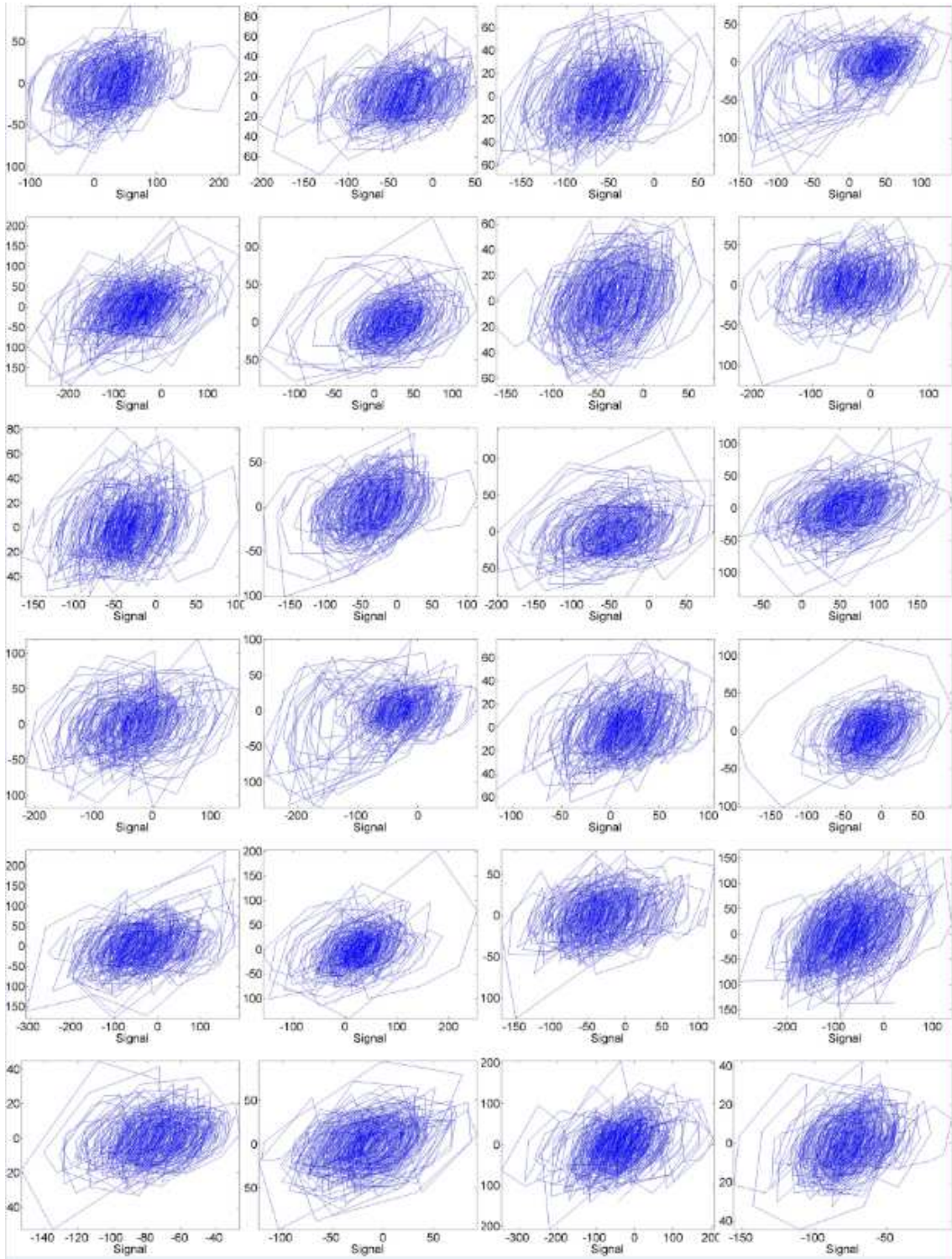


Figure 9: Phase Portraits for 24 samples of EEG recorded during normal activity from non-epileptogenic region

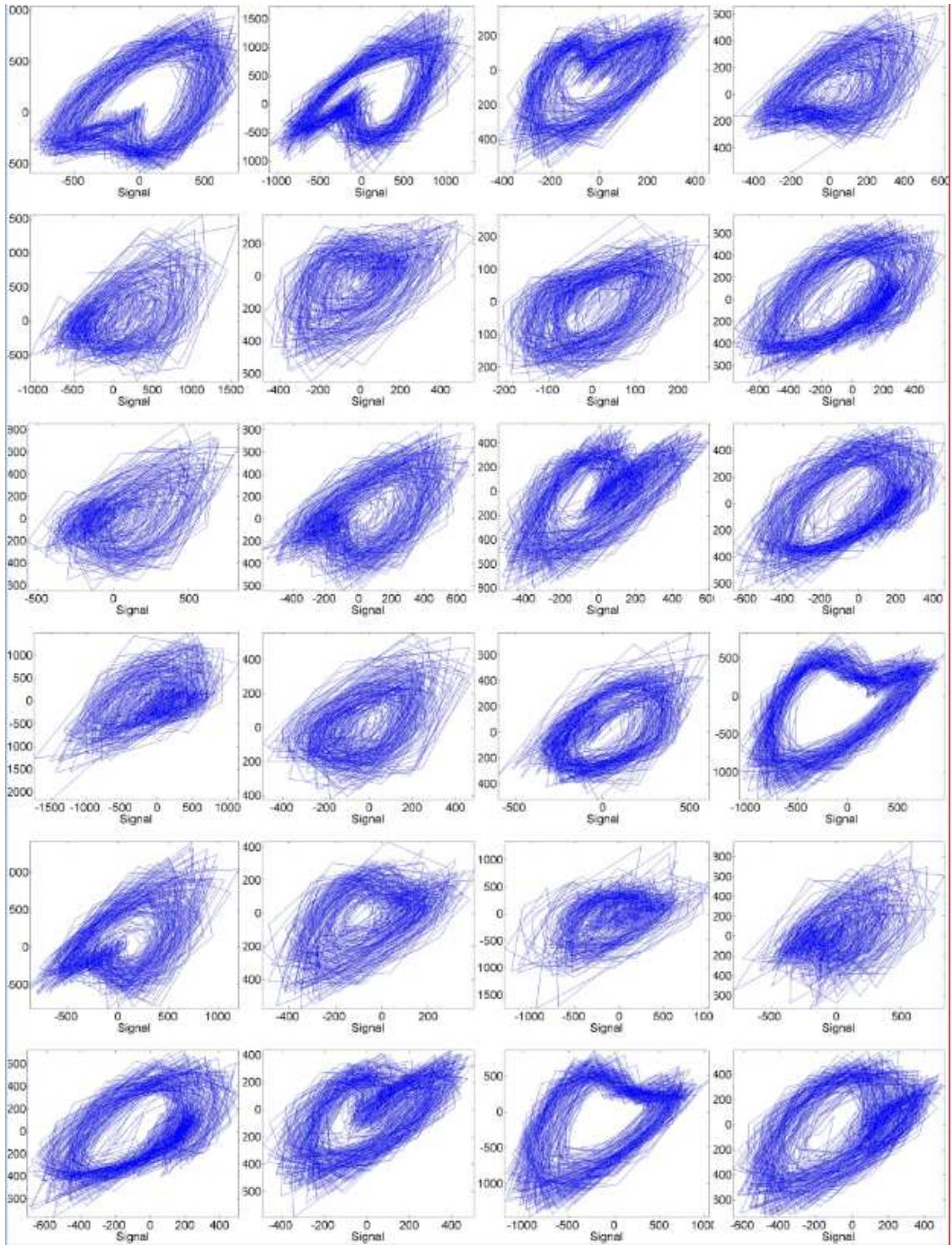


Figure 10: Phase Portraits for 24 samples of EEG recorded during seizure activity from epileptogenic region

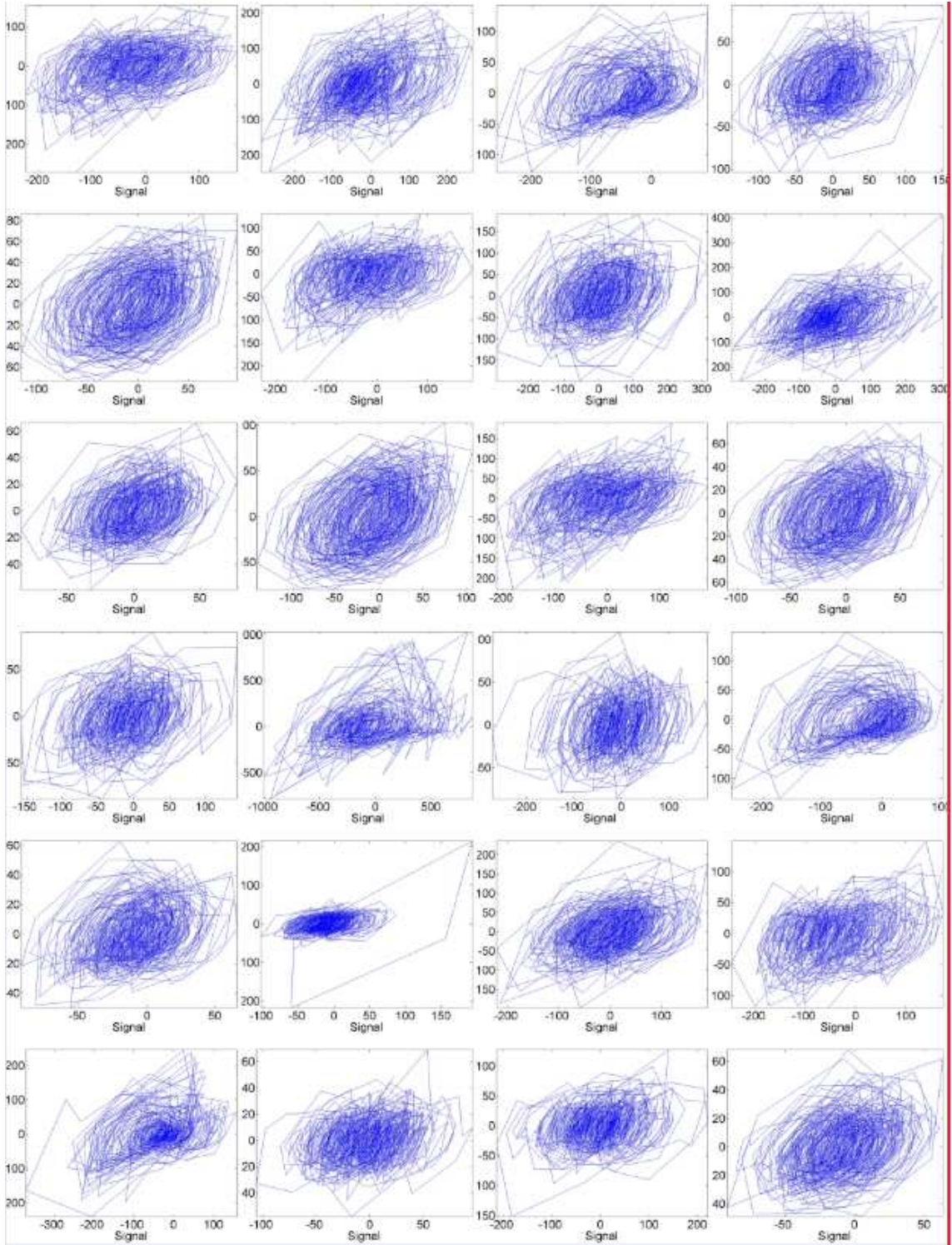


Figure 11: Phase Portraits for 24 samples of EEG recorded during normal activity from epileptogenic region

## 4. Conclusion

After describing the formulation of a hyperbolic secant based solitary wavelet with vanishing higher moments translating to efficient detection of burst type signals, the present paper presents the spectral and nonlinear analyses results of EEG data taken from the Klinik für Epileptologie database. Specifically, from the Fourier Spectral Analysis, it is seen that Seizure EEG spectra have well-defined high frequency peaks, characteristic of resonance dominance, whereas healthy EEG spectra are much more uniformly spread out across a wide range of frequencies, with the only dominant peak seen in the central frequency. However, Non-Seizure Epileptogenic EEG spectra followed trends of Seizure EEG spectra, albeit with high frequency peaks closer to the central frequency. The solitary wavelet analysis results indicate a high degree of localization of Seizure EEG data, with dominant scales hardly exceeding 8, whereas analysis of healthy EEG show a much wider range of dominant scales, extending all the way up to 100 and beyond. Non-Seizure Epileptogenic EEG wavelet analysis indicate localized scale dominance in the range between 8 and 22. Following this, nonlinear analysis for the three datasets are presented, where phase portraits for Seizure EEG are seen to display periodic orbits characteristic of resonant behavior, whereas phase portraits for Healthy and Non-Seizure Epileptogenic EEG are much more ergodic. Finally, it is seen that the Fractal Dimension (D) and Lyapunov Exponent (LLE) values for Seizure EEG are much lower than the Healthy EEG counterparts, with negative LLE values seen for some EEG samples. The D and LLE values of Non-Seizure Epileptogenic EEG are obtained in between those of the healthy and seizure counterparts, indicating a lower dimensionality and chaoticity than normal, yet higher than those of seizure EEG. Thus, in essence, the results presented in this paper clearly highlight the fact that a distinct and uniquely identifiable low-dimensional chaotic behavior is observed in the case of EEG taken from Epileptogenic region, during non-seizure activities. This information can be used both as a preventive epilepsy diagnostic technique, as well as a post-surgical recovery assessment tool, and this forms the novelty of the present work.

## References

- [1] M. Ausloos, M. Diricx, *The Logistic Map and the Route to Chaos: From the Beginnings to Modern Applications*, (Springer, US, 2006).
- [2] S. H. Strogatz, *Nonlinear Dynamics and Chaos: With Applications to Physics, Biology, Chemistry, and Engineering*, (Westview Press, Cambridge, 2008).
- [3] F. Cramer, *Chaos and Order the Complex Structure of Living Systems*. (Springer, 1993).
- [4] D. S. Coffey, *Self-organization, complexity and chaos: the new biology for medicine*. Nature medicine **4**, 882-885 (1998).
- [5] G. Contopoulos, *Order and chaos in dynamical astronomy*, (Springer Science and Business Media, 2002).
- [6] J. Laskar, *Large-scale chaos in the solar system*, Astronomy and Astrophysics **287**, L9-L12 (1994).
- [7] A. B. Cambel, *Applied chaos theory-A paradigm for complexity*. (Academic Press, Inc., 1993).
- [8] K. Aihara, *Chaos engineering and its application to parallel distributed processing with chaotic neural networks*. Proceedings of the IEEE, **90** 919-930 (2002).
- [9] G. Chen, *Controlling chaos and bifurcations in engineering systems*. (CRC press, 1999).
- [10] R. B. Stull, *An introduction to boundary layer meteorology*. (Springer Science and Business Media, 1988).
- [11] M. F. Barnsley, A. D. Sloan, *Chaotic Compression*, Computer Graphics World, **3** (1987).
- [12] K. E. Barner G. R. Arce, *Nonlinear Signal and Image Processing: Theory, Methods, and Applications*, (CRC Press, U.S, 2003).
- [13] S. Saini, J. S. Saini. *Secure communication using memristor based chaotic circuit*. Parallel, Distributed and Grid Computing (PDGC), 2014 International Conference on. IEEE, (2014).
- [14] S. Shaerbafe, S. A. Seyedin. *Nonlinear Multiuser Receiver for Optimized Chaos-Based DS-CDMA Systems.*, Iranian Journal of Electrical and Electronic Engineering **7**, 149 (2011): 149.
- [15] L. Kocarev, *From chaotic maps to encryption schemes*. Circuits and Systems, (1998).
- [16] G. Jakimoski, L. Kocarev. *Chaos and cryptography: block encryption ciphers based on chaotic maps*. IEEE Transactions on Circuits and Systems I: Fundamental Theory and Applications **48** 163-169 (2001).
- [17] R. B. Govindan, K. Narayanan, M. S. Gopinathan. *On the evidence of deterministic chaos in ECG: Surrogate and predictability analysis*, Chaos: An Interdisciplinary Journal of Nonlinear Science **8**, 495-502, (1998).
- [18] D. E. Albert, *Chaos and the ECG: fact and fiction*, Journal of electrocardiology, **24**, 102-106, (1991).
- [19] W. S. Pritchard, D. W. Duke, *Measuring chaos in the brain: a tutorial review of nonlinear dynamical EEG analysis*, International Journal of Neuroscience, **67**, 31-80, (1992).
- [20] S.A.R.B. Rombouts, R.W.M. Keunen, C.J. Stam, *Investigation of nonlinear structure in multichannel EEG*, Phys. Lett. A **202**, 352 (1995).
- [21] A.C.K. Soong C.I.J.M. Stuart, *Evidence of chaotic dynamics underlying the human alpha-rhythm electroencephalogram*, Biol. Cybern. **62**, 55 (1989).
- [22] J. Jeong, M.S. Kim, S.Y. Kim, *Test for low-dimensional determinism in electroencephalograms*, Phys. Rev. E **60**, 831 (1999).
- [23] A. Babloyantz, J.M. Salazar, and G. Nicolis, *Investigation of nonlinear structure in multichannel EEG*, Phys. Lett. A **111**, 152 (1985).
- [24] P. Achermann, R. Hartmann, A. Gunzinger, W. Guggenbuhl, A.A. Borbely, *Investigation of EEG non-linearity in dementia and Parkinson's disease*, Electroencephalogr. Clin. Neurophysiol. **90**, 384, (1994).
- [25] C.J. Stam, T.C.A.M. van Woerkom, W.S. Pritchard, *Use of non-linear EEG measures to characterize EEG changes during mental activity*, Electroencephalogr. Clin. Neurophysiol. **99**, 214, (1996).
- [26] J. Theiler P. Rapp, *Indications of nonlinear deterministic and finite-dimensional structures in time series of brain electrical activity: Dependence on recording region and brain state*, Electroencephalogr. Clin. Neurophysiol. **98**, 213, (1996).
- [27] P.E. Rapp, T.R. Bashore, J.A. Martinerie, A.M. Albano, I.D. Zimmermann, A.I. Mees, *Dynamics of brain electrical activity*, Brain Topogr. **2**, 99 (1989).

- [28] C.L. Ehlers, J. Havstad, D. Prichard, J. Theiler, *Low doses of ethanol reduce evidence for nonlinear structure in brain activity* J. Neurosci. 18, 7474, (1998).
- [29] J. Jeong, T.H. Chae, S.Y. Kim, S.H. Han, *Nonlinear dynamic analysis of the EEG in patients with Alzheimer's disease and vascular dementia*, J. Clin. Neurophysiol. 18, 58, (2001).
- [30] C.J. Stam, T.C.A.M. van Woerkom, R.W.M. Keunen, *Non-linear analysis of the electroencephalogram in Creutzfeldt-Jakob disease*, Biol. Cybern. 77, 247, (1997).
- [31] J.-L. Nandrino, L. Pezard, J. Martinerie, F. El Massioui, B. Renault, R. Jouvent, J.-F. Allilaire, and D. Wildlocher, *Decrease of complexity in EEG as a symptom of depression*, NeuroReport 5, 528, (1994).
- [32] P. Kirsch, C. Besthorn, S. Klein, J. Rindfleisch, R. Olbrich, *Indications of nonlinear deterministic and finite-dimensional structures in time series of brain electrical activity: Dependence on recording region and brain state*, Brain Topogr 2, 187, (1990).
- [33] K. Lehnertz C.E. Elger, *Can epileptic seizures be predicted? Evidence from nonlinear time series analysis of brain electrical activity*, Phys. Rev. Lett. 80, 5019, (1998).
- [34] M.C. Casdagli, L.D. Iasemidis, R.S. Savit, R.L. Gilmore, S. Roper, J.C. Sackellares, *Nonstationarity in epileptic EEG and implications for neural dynamics*, Electroencephalogr. Clin. Neurophysiol. 102, 98, (1997).
- [35] R.G. Andrzejak, G. Widman, K. Lehnertz, C. Rieke, P. David, C.E. Elger, *Indications of nonlinear deterministic and finite-dimensional structures in time series of brain electrical activity: Dependence on recording region and brain state*, Epilepsy Res. 44, 129, (2001).
- [36] J. Theiler, *On the evidence for low-dimensional chaos in an epileptic electroencephalogram*, Phys. Lett. A 196, 335, (1995).
- [37] F. Mormann, K. Lehnertz, P. David, C.E. Elger, *Mean phase coherence as a measure for phase synchronization and its application to the EEG of epilepsy patients*, Physica D 144, 358, (2000).
- [38] J. Martinerie, C. Adam, M. Le Van Quyen, M. Baulac, S. Clemenceau, B. Renault, and F.J. Varela, *Epileptic seizures can be anticipated by non-linear analysis*, Nat. Med. 4, 1173 (1998).
- [39] K. Lehnertz, J. Arnhold, P. Grassberger, C. E. Elger, *Chaos in Brain?* (World Scientific, Singapore, 2000).
- [40] L.D. Iasemidis, J.C. Sackellares, H.P. Zaveri, W.J. Williams, *Phase space topography and the Lyapunov exponent of electrocorticograms in partial seizures*, Brain Topogr. 2, 187, (1990).
- [41] R. S. Fisher, *Epileptic seizures and epilepsy: definitions proposed by the International League Against Epilepsy (ILAE) and the International Bureau for Epilepsy (IBE)*, Epilepsia, 46, 470-472 (2005).
- [42] R. S. Fisher, *ILAE official report: a practical clinical definition of epilepsy*, Epilepsia, 55, 475-482, (2014).
- [43] T. Stokes, *Clinical guidelines and evidence review for the epilepsies: diagnosis and management in adults and children in primary and secondary care*, London: Royal College of General Practitioners, 397 (2004).
- [44] J. R. Hughes, *Absence seizures: a review of recent reports with new concepts*, Epilepsy and Behavior, 15 404-412, (2009).
- [45] R. G. Andrzejak, *Indications of nonlinear deterministic and finite-dimensional structures in time series of brain electrical activity: Dependence on recording region and brain state*, Physical Review E 64, 061907 (2001).
- [46] A. Babloyantz, A. Destexhe, *Low-dimensional chaos in an instance of epilepsy*, Proceedings of the National Academy of Sciences 83, 3513-3517 (1986).
- [47] D. R. Larson. *Wavelet Analysis and Applications*, Birkhauser, (2007).
- [48] I. Daubechies. *Different Perspectives on Wavelets*, American Mathematical Society, (1993).
- [49] M. Weeks. *Digital Signal Processing using MATLAB and Wavelets*, Jones and Bartlett, (2011).
- [50] Y.S. Kivshar, G. Agrawal, *Optical Solitons: From Fibers to Photonic Crystals.*, (USA: Academic Press, 2013).
- [51] A. Kudrolli, A. J. P. Gollub. *Patterns and spatiotemporal chaos in parametrically forced surface waves: a systematic survey at large aspect ratio*. Physica D: Nonlinear Phenomena **97**, 133-154 (1996).
- [52] J. Briggs, *Fractals: The patterns of chaos: A new aesthetic of art, science, and nature*. (Simon and Schuster, 1992).
- [53] M. Lakshmanan, S. Rajaseekar, *Nonlinear dynamics: integrability, chaos and patterns*. (Springer Science and Business Media, 2012).
- [54] I R. Epstein, K. Showalter. *Nonlinear chemical dynamics: oscillations, patterns, and chaos*. The Journal of Physical Chemistry *100* 13132-13147 (1996).
- [55] R. Gilmore, M. Lefranc, *The Topology of Chaos*, (Wiley,US, [2002]).
- [56] J. M. T. Thompson, H. B. Stewart, *Nonlinear Dynamics and Chaos* (Wiley,UK, [2002]).
- [57] P. Maragos, F. K. Maragos, F.K.Sun, Petros, Fang-Kuo Sun, *Measuring the fractal dimension of signals: morphological covers and iterative optimization*, IEEE Trans. Signal Processing, 41, 108-121, (1993).
- [58] R. G. James, K. Burke, J. P. Crutchfield, *Chaos forgets and remembers: Measuring information creation, destruction, and storage*, Int. J Bifurcation Chaos. **378**, 2124 (2014).
- [59] M. T. Rosenstein, J. J. Collins, C. J. De Luca, *A practical method for calculating largest Lyapunov exponents from small data sets*, Physica D, **65**, 117, (1993).